Experimental Study on Confined Two-Phase Jets

D. Albagli* and Y. Levy†
Technion—Israel Institute of Technology, Haifa, Israel

The basic mixing phenomena in confined, coaxial, particle-laden turbulent flows are studied within the scope of ram combustor research activities. Cold-flow experiments in a relatively simple configuration of confined, coaxial two-phase jets provided both qualitative and quantitative insight on the multiphase mixing process. Pressure, tracer gas concentration, and two-phase velocity measurements revealed that unacceptably long ram combustors are needed for complete confined jet mixing. Comparison of the experimental results with a previous numerical simulation displayed a very good agreement, indicating the potential of the experimental facility for validation of computational parametric studies.

Introduction

THE ram rocket is considered to be one of the most promising concepts in the field of air-breathing supersonic missiles. This propulsion system consists of a primary combustion chamber, where fuel-rich, metallized solid propellants are burned and expanded through a primary nozzle into a ram combustor. The primary combustion products, containing partly unreacted gaseous fuels and metal particles, mix and react with secondary ram air in the ram combustor and are exhausted through a secondary nozzle.

The two-phase flowfield in ram combustors determines the extent of mixing between the fuel-rich primary exhaust and the secondary ram air, which, in turn, significantly affects the secondary combustion efficiency. The objective of this study was to develop an experimental system for the measurement of the two-phase flowfield in a simulated ram combustor environment and to evaluate a numerical simulation that was developed to pursue the same goal. Experimental results were also required to determine the boundary conditions for the computer code simulating specific operating conditions.

The ability to deal with the complex flowfield in a ram combustor environment requires rigorous knowledge of a number of physicochemical processes, including turbulent mixing of the gas generator exhaust with the ram air, recirculating flow, finite-rate chemical kinetics of gaseous fuels, and particulate fuel ignition and combustion. Studies on ram combustor geometry and performance were published by a number of authors, e.g., Schadow,[1-3] Schadow et al.,[4] Smoot and Anderson,[5] Smoot and Fort,[6] Miller et al.,[7] Choudhury,[8] Streby,[9] Ishikawa,[10] and Stull et al.[11] These works range from cold-flow water tunnel simulations to combustion characteristics of particle-laden flows, but drawing general conclusions is difficult because of their project-specific nature. Theoretical studies on confined jets, leading to the basic ram combustor configuration, were carried out by Curtet,[12] Chigier and Beér,[13] Peters et al.,[14] Ghia et al.,[15] Tufts and Smoot,[16] and Razinsky and Brighton.[17] Most of these analyses are based on the boundary-layer approach, often revealing good agreement with experimental data and showing the predominance of viscous effects in ducted mixing systems. The incorporation of the particulate phase in such flowfields comprising all types of interaction with the host phase has not yet been achieved despite the attempts of Migdal and Agosta,[18] Genovese et al.,[19] and DiGiacinto et al.,[20] which preclude certain interphase coupling effects.

The physical model implemented in a previous publication of the authors[21] predicted the mixing characteristics of particle-laden, confined, coaxial, turbulent jets with coupled mass transport, dynamic and thermal nonequilibrium effects in a simulated ram combustor. The equations governing the flow of both gas and particle phases were assessed according to the Eulerian approach. The first of the two ram combustor simulations described in the previous work, characterized by low speed, cold flow of confined two-phase jets, is the counterpart of the present study.

Conducting an experimental investigation on the flowfield in a ram combustor is extremely difficult because of the hostile environment of high temperature, high pressure, nontransparent two-phase flow. Basic studies for understanding the governing mechanisms of specific phenomena are therefore confined to simplified experimental models. According to this methodology, the present work forcuses on the mixing process in particle-laden, ducted, concentric, turbulent jets.

The velocity measurements involve complicated techniques to satisfy the needs of the experimental study. The required data are the local instantaneous velocity histograms of the two phases. The mean and fluctuating velocity values can then be evaluated from these histograms. The measurement technique selected was Laser Doppler Velocimetry (LDV), which enables tracing of velocities of particles scattered in the host fluid.[22] In the case of two-phase flow, two types of particles are simultaneously present. The fine (tracking) particles that follow the flow and reveal the instantaneous velocity of the host fluid and the larger ones that represent the discrete phase and have their own trajectories. One of the great advantages of the LDV technique is that it supplies, with certain modifications, simultaneous information on the velocity and the size of an individual particle. The information on the size of the particle is obtained from the shape of the signal recorded by one or more photodetectors and is affected by the properties of the particle and by the specific technique used.[23,24]

The particles can be classified in two groups according to their shape. Spherical particles with smooth surface (liquid drops, gas bubbles, etc.) and those of arbitrary shape and optical characteristics (sand, powders, etc.).

Two major techniques exist to date that are appropriate for size measurements. The Phase Doppler Anemometry (PDA) is suitable for measuring the diameter of particles of the first group having diameters $> \sim 3\ \mu m$.[25-30] The technique is based on interferometric phenomena caused by transparent spheres crossing the LDV control volume. It is independent of particle trajectories as well as insensitive to light intensity. The particle diameter can be obtained with a relative error of $< 5\%$.

Arbitrary shaped particles of various refractive indices that

Received Oct. 18, 1989; revision received May 17, 1990; accepted for publication May 22, 1990.

*Graduate Student, Faculty of Aerospace Engineering.
†Senior Lecturer, Faculty of Aerospace Engineering. Member AIAA.

form the second group can be measured by the pedestal amplitude method. This method is based on the relation between the size of the particle and the pedestal amplitude of its signal.[23,24,31–37] It is associated with the absolute intensity of the signal and thus depends on the particle's trajectory in the control volume (which has a Gaussian light intensity distribution); therefore, it requires calibration for every optical setup. The accuracy of the pedestal technique is lower than that of the PDA, with a measurement error up to 30%. This accuracy can be increased to some extent if measurements are limited to areas where the intensity of the laser light in the control volume is uniform.

Data obtained by either of the described techniques are subsequently arranged in groups of identical size and velocity range and processed to form a two-dimensional size/velocity histogram. Detailed patterns of the local two-phase flow can be reconstructed by means of such histograms.

In the special case of two-phase flow comprising particles of uniform size distribution, a much easier approach can be adopted. The tracking particles representing the continuous phase are typically much smaller than the discrete phase particles. Hence, only two groups of particles simultaneously exist in the flow, with corresponding signal amplitudes of different orders of magnitude. By imposing a variable threshold level on the photodetector output, one can distinguish between the scattered light originating from large discrete particles and that from the fine tracking particles.

Experimental Investigation

The major objective of the experimental program was to obtain a general insight on the mixing phenomena in the initial region of confined, concentric, chemically inert two-phase jets by measurement of pressure, concentration, and two-phase velocity distributions.

Experimental System

A schematic diagram of the experimental test section is shown in Fig. 1. The external tube, simulating the ram combustor, had a length of 1.43 m and an inner diameter of 103 mm with a wall thickness of 3 mm. Two geometrically identical external tubes were used during the experiments: a polyvinyl chloride (PVC) tube for pressure and concentration, and a glass tube for velocity measurements. The internal tube had an inner diameter of 14 mm with a wall thickness of 1 mm. It was centered by means of three symmetrically placed slender rods.

The primary (internal) airflow was supplied by a 20-MPa pressure line drawn from storage vessels through a manually operated valve. The primary mass flow rate was in the range of 15–50 g/s and was measured with a calibrated choked nozzle.

The secondary (external) airflow was supplied by means of a blower that could deliver up to 0.6 kg/s at a head of 8.8 kPa (900-mm water). The airflow was controlled by a flap-type valve mounted at the blower exit. The actual flow rate was measured by means of a standard orifice (BS 1042) farther downstream of the 150-mm-diam supply line. The secondary air was directed to the test section after having passed through a settling chamber, thus acquiring a more uniform velocity profile.

Carbon dioxide was used as tracer gas during the concentration measurements in order to determine the mixing characteristics of the two coflowing concentric streams. A 10-MPa CO_2 bottle was connected to the primary airflow by means of a 25-mm-diam pipe and its mass flow rate was controlled by a calibrated valve/choked nozzle combination. This enabled the strict determination of the tracer gas mass fraction in the primary air.

To allow for continuous seeding of the flow during LDV measurements, a particle seeder was built implementing the fluidized bed principle. A mixture of 5- and 20-μm-mean-diam aluminum oxide particles, available from Buehler Ltd. was used for seeding. The smaller particles were assumed to follow the gaseous phase while the bigger ones simulated the discrete particle phase. Since these particles were prone to agglomeration due to humidity and electrostatic forces, it was necessary to disperse them well before they joined the main flow. Therefore, special attention was focused on getting a proper dispersion of particles from the seeder (Fig. 2). The particles were introduced to a fluidized bed through a screw feeder actuated by a variable-speed dc motor. A transparent plexiglass tube with volumetric scale was mounted on the top of the particle container to enable evaluation of the average particle mass flow rate. The bed material in the fluidized bed consisted of 0.7-mm glass beads located on a dense air filter used as the distributor. The air required for fluidization was taken from a 0.6-MPa pressure line and passed through a control valve and a choked nozzle to allow flow rate measurements. This flow rate was deducted from the main flow rate in order to keep experimental conditions constant. Another motor with a rotating eccentric weight was mounted on the main body to generate vibrations for better dispersion of particles.

Experimental Procedure

The experimental conditions are summarized in Table 1. They were selected to match those of the numerical simulation

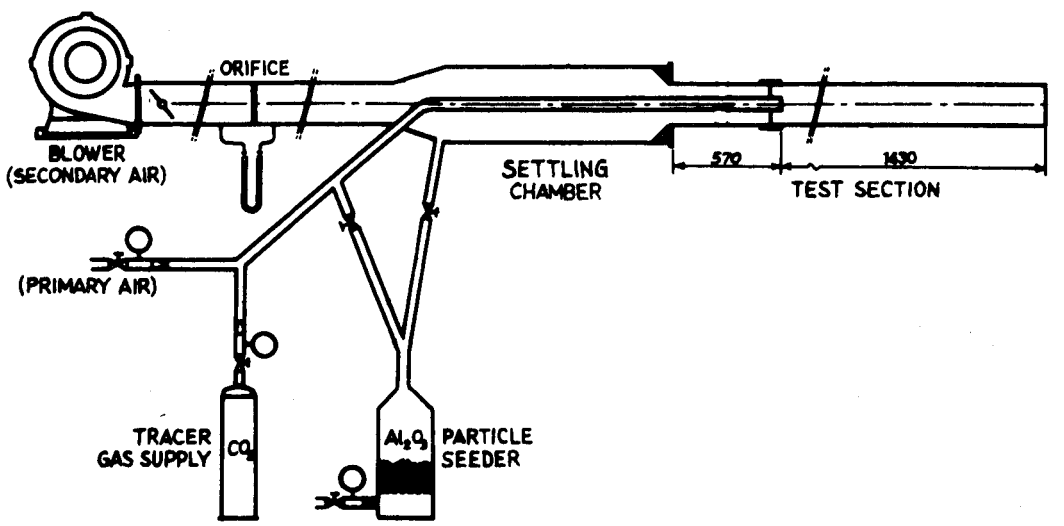

Fig. 1 Experimental setup.

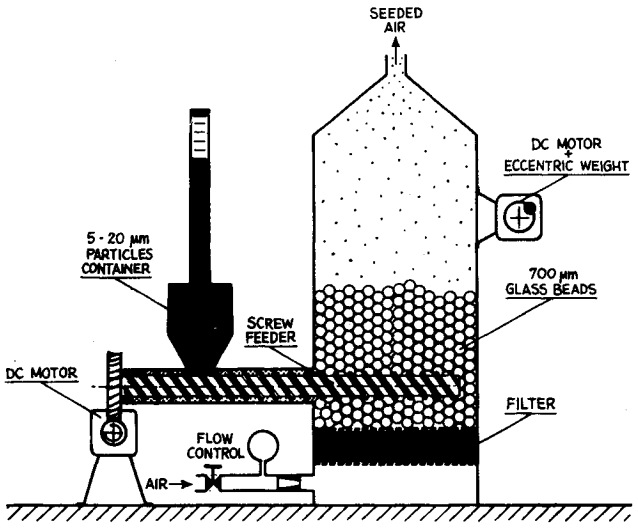

Fig. 2 Particle seeder.

described in Albagli and Levy[21] to facilitate validation of the predicted values.

Measurement of Wall Pressure Distribution

Fifteen static pressure taps were distributed along the external tube at an initial axial spacing of 40 mm and a stretching factor of 1.1 (Fig. 3). The pressure, sensed at 1-mm-diam holes, was transmitted to a multimanometer held at a slope of 15 deg, quadrupling the reading precision. Difficulties encountered during the measurements emanated mainly from strong fluctuations in the initial region and entailed time averaging.

Measurement of CO_2 Mass Fraction Distribution

In addition to the pressure taps, 8-mm-diam ports were drilled at each measurement station to enable the accommodation of concentration probes (Fig. 3). The probes were made of 1-mm-i.d. and 2-mm-o.d., L-shaped stainless steel tubes. A suction pump equipped with a rotameter was used to ensure on-line isokinetic sampling of the gas in coordination with the local velocity measured by a pitot-static tube. The gas chromatography technique was used for the analysis of the gas samples. Details of this technique can be found in Chedaille and Braud.[38] A Philips PV-4000 series chromatograph was implemented for gas analysis, which required a continuous helium supply of 3 l/h, monitored by means of a bubble flow meter. For 100°C column temperature, the time needed for the analysis of each 4-cc gas sample was about 10 min. Because of steep radial gradients and strong fluctuations in the mixing layer, the determination of precise radial concentration profiles was practically impossible. Two sets of measurements were performed: one along the main axis and one at a radial distance equal to the inner tube radius. Chromatograms were both plotted by an analog recorder for manual data processing and transmitted to a PDP 11/84 minicomputer for automatic mass fraction calculations.

Table 1 Experimental conditions

Pressure	100 kPa
Temperature	300 K
External air velocity	22.5 m/s
Internal air velocity	42.5 m/s
Internal particle velocity	41.4 m/s
Internal CO_2 mass fraction	0.10
Particle mean diameter	20 μm
Diameter ratio	0.135
Mass flow ratio	0.035
Momentum ratio	0.066
Average Reynolds number	1.4×10^5

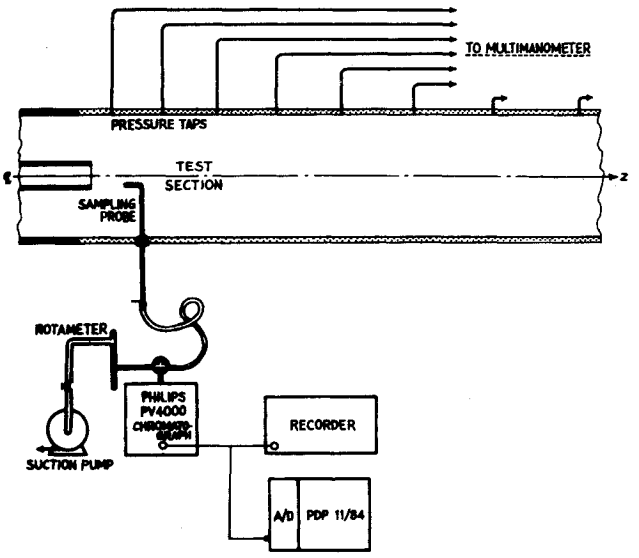

Fig. 3 Gas sampling and analysis system.

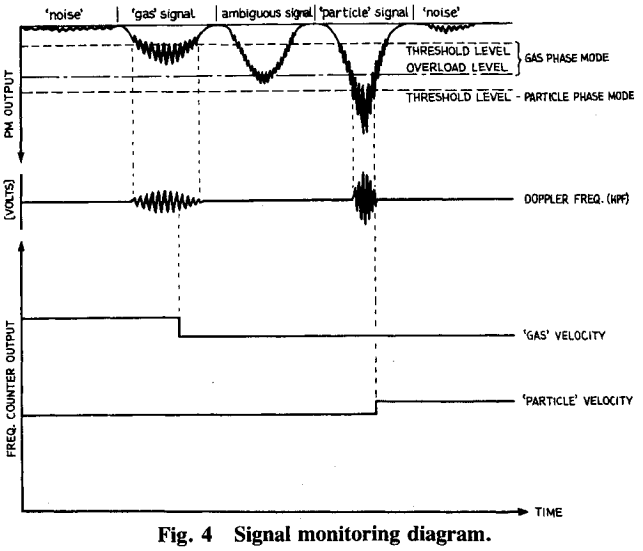

Fig. 4 Signal monitoring diagram.

Measurement of Axial Velocity Profiles

The LDV technique was implemented for the measurement of both gas and particle phase velocities. The discrimination of signals originating from particles of bimodal size distribution forming the continuous (5-μm particles) and discrete (20-μm particles) phases was achieved by means of the pedestal technique. The problem of cross talk between the phases, where the signal amplitude of a large particle passing through the edge of the probe volume might be of the same order as that of a small particle crossing the center of the probe volume, was insignificant in this study, owing to the large difference between signals originating from the two phases. The reduction of the acceptable signal zone in the control volume to ~60 μm in diameter, by means of the pinhole in the photodetector, decreased the intensity differences within the effective control volume. The signal monitoring diagram is shown in Fig. 4. The threshold and overload levels of the LDV counter were set in accordance with the photodetector signal monitored at the scope. For gas phase sampling, the threshold level was set slightly over the photomultiplier noise level, whereas the overload level was above the maximum possible signal amplitude of a gas particle (5-μm). For discrete phase (20-μm) sampling, the setting of the threshold level well over the maximum signal amplitude of a gas particle together with the inactivation of the overload level control was required.

Figures 5 and 6 show the velocity histograms of the processed signals from the counter output. By proper adjustment of the threshold level, the particle phase local velocity prob-

ability distribution histogram was obtained as shown in Fig. 5. When the threshold level was reduced to the noise level without adequate setting of the overload level, both gas and particle phase velocity histograms were obtained together, as in Fig. 6. Unfortunately, the frequent overlapping of the two histograms prevented the graphic discrimination of the phases.

The schematic of the LDV system used during the experiments is shown in Fig. 7. A 15-mW He-Ne laser (Spectra Physics Model 120S) was directed to an LDV modular optics unit (DISA 55X) and separated into two parallel coherent beams of equal intensity. These beams were then focused by a planoconvex imaging lens of 300-mm focal length to their intersection region where an ellipsoidal control volume was formed, as seen in the inset of Fig. 7. Scattered light from particles crossing the control volume was collected and focused on the 150-μm pinhole of the photomultiplier (DISA 55X) by a combination of two biconvex lenses of 250- and 80-mm focal length. Two plane mirrors, before the imaging lens and after the first collecting lens, were used to yield a compact optical setup. The main characteristics of the LDV system are summarized in Table 2.

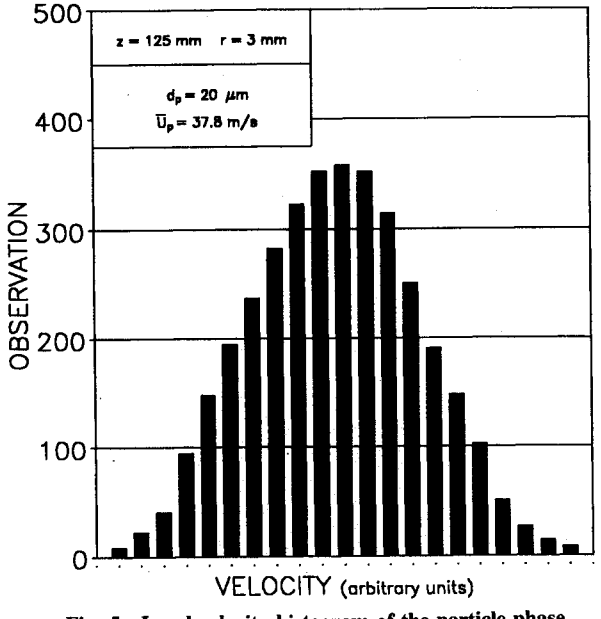

Fig. 5 Local velocity histogram of the particle phase.

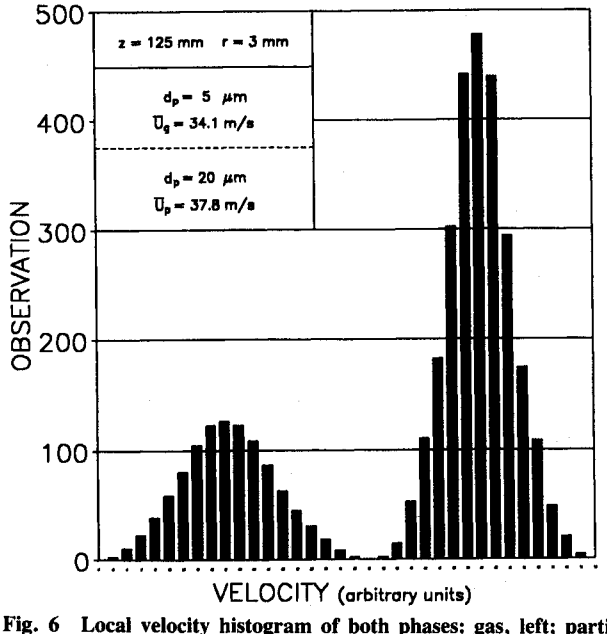

Fig. 6 Local velocity histogram of both phases: gas, left; particle, right.

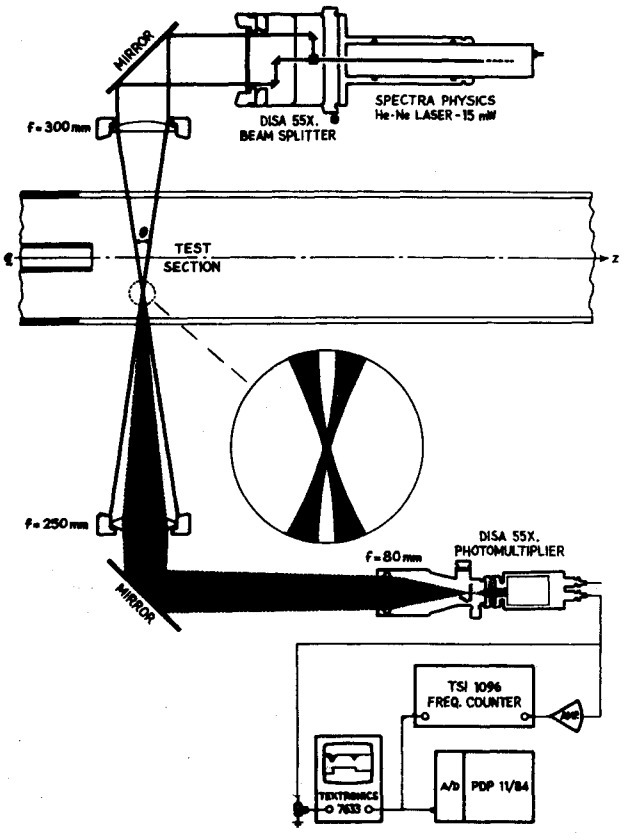

Fig. 7 LDV measurement system.

Table 2 Characteristics of the Laser Doppler Velocimetry system

He-Ne laser wavelength	632.8 μm
Laser beam diameter at e^{-2} intensity level	1.1 mm
Half angle of intersection	5.9 deg
Probe volume length	600 μm
Probe volume diameter	61 μm
Pinhole diameter	150 μm
Fringe spacing	3.1 μm
Number of fringes seen at the pinhole	20
Magnification of the collecting optics	2.45
Velocimeter constant	3.08 m/s/MHz

The electrical signal generated by the photodetector was transmitted to an LDV counter unit (TSI Model 1096 LDA Signal Processor System), which produced analog signals proportional to the Doppler frequency. The counter analog output was connected to a 12-bit A/D converter interfaced with a PDP 11/84 minicomputer. The software for sampling, data reduction, and statistical analysis was self-developed and implemented with success.

The comparator accuracy of the LDV counter unit that determined the maximum allowable error in the frequency measurements was usually set to 2%. In regions where the signal-to-noise ratio was relatively low (e.g., near the walls), it was set to a maximum of 5%. The validated data rate of the counter was on the order of 1000 particles/s. The analog output was sampled at a relatively low frequency of 100 Hz, revealing a validated data rate/sampling rate ratio on the order of 10, in order to reduce velocity bias error. A population of 5000 samples was collected at each point, requiring an acquisition and processing time of about 1 min. The digitized raw data were first filtered from repetitive identical velocity readings, then points outside the range of three times the standard deviation from the mean value (which covers ~99.7% of the population, assuming Gaussian probability distribution) were eliminated. The resulting velocity histogram and mean and fluctuating velocity components were obtained by means of the interactive software.

Results and Discussion

The main results of the experimental investigation are presented in Figs. 8–15. These comprise pressure, tracer gas concentration (mass fraction), and two-phase velocity measurements. The predicted values of the corresponding variables described in Albagli and Levy[21] are superimposed in these figures for convenience.

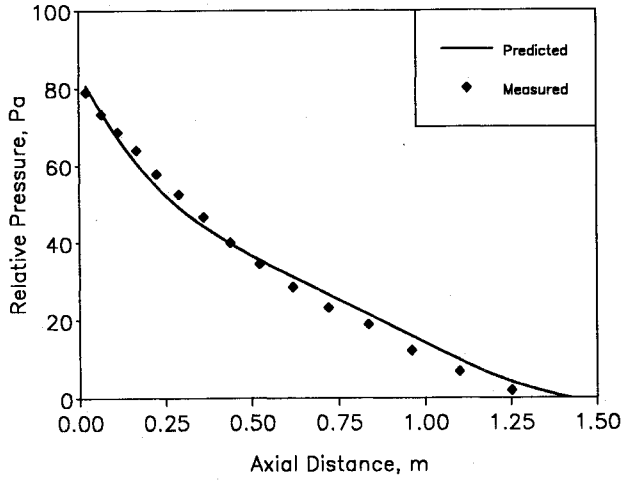

Fig. 8 Measured vs predicted wall pressure distribution.

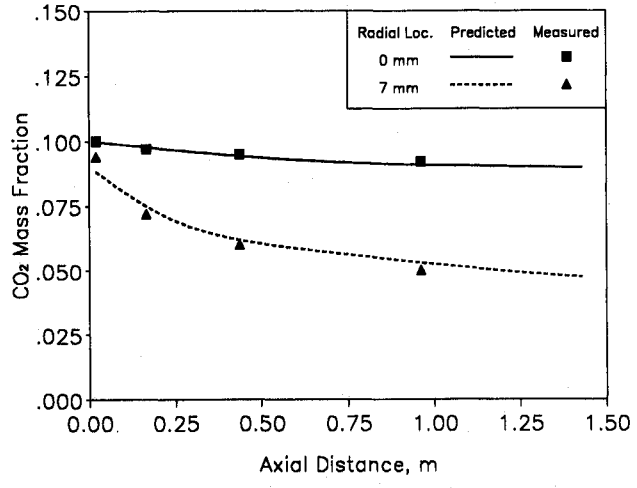

Fig. 9 Measured vs predicted CO_2 mass fraction distributions.

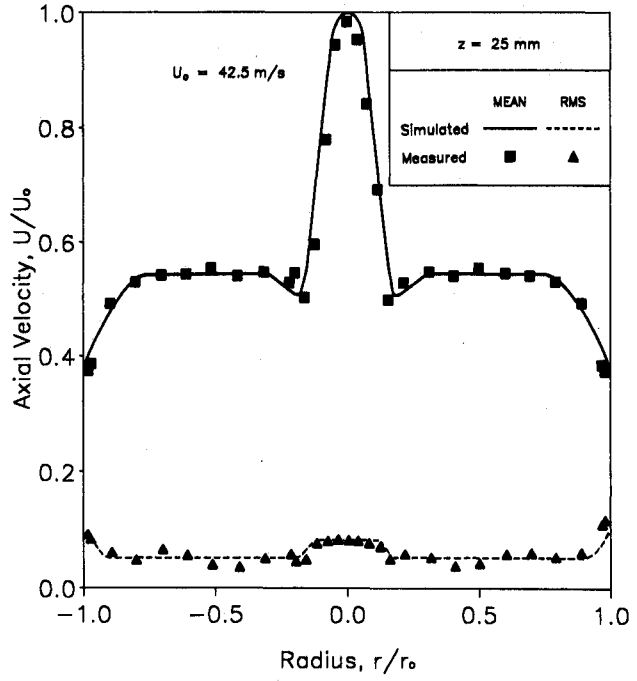

Fig. 10 Measured gas phase velocity profiles at z = 25 mm.

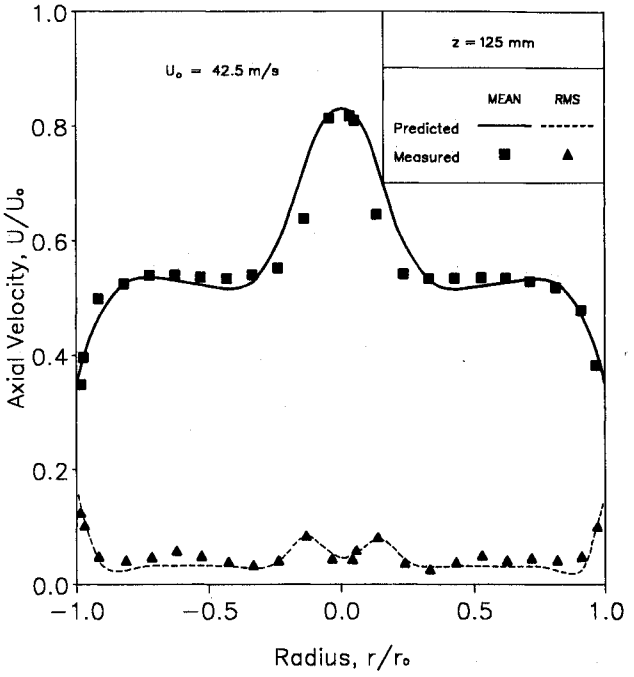

Fig. 11 Measured vs predicted gas phase velocity profiles at z = 125 mm.

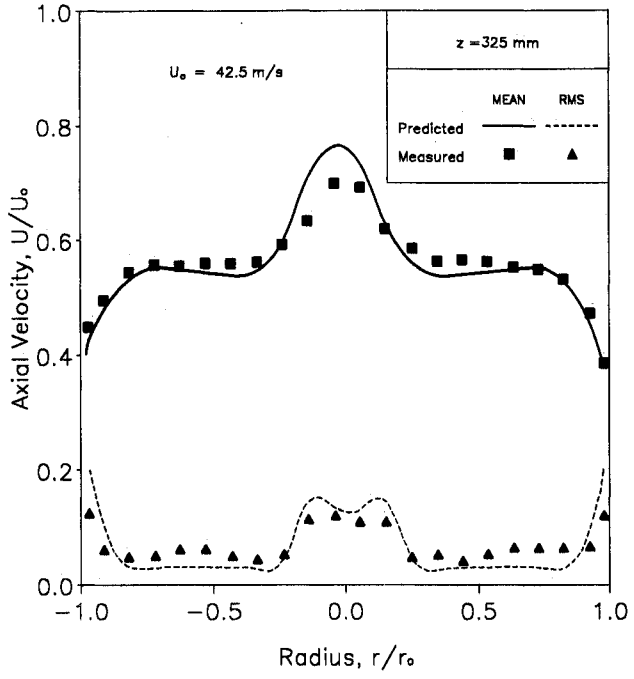

Fig. 12 Measured vs predicted gas phase velocity profiles at z = 325 mm.

The measured wall pressure distribution in the combustor model is shown in Fig. 8, together with the predicted profile. A good agreement between the measured and predicted absolute values is obtained. The slight discrepancies toward the combustor outlet may be attributed to the inadequacy of the prescribed exit conditions in the numerical simulation, which assumed absence of axial gradients.

The measured CO_2 mass fraction distributions comply well with the predicted values, as seen in Fig. 9. Centerline (r = 0) CO_2 concentration decay is predicted better than that within the mixing layer (r = 7 mm), possibly because of the relatively

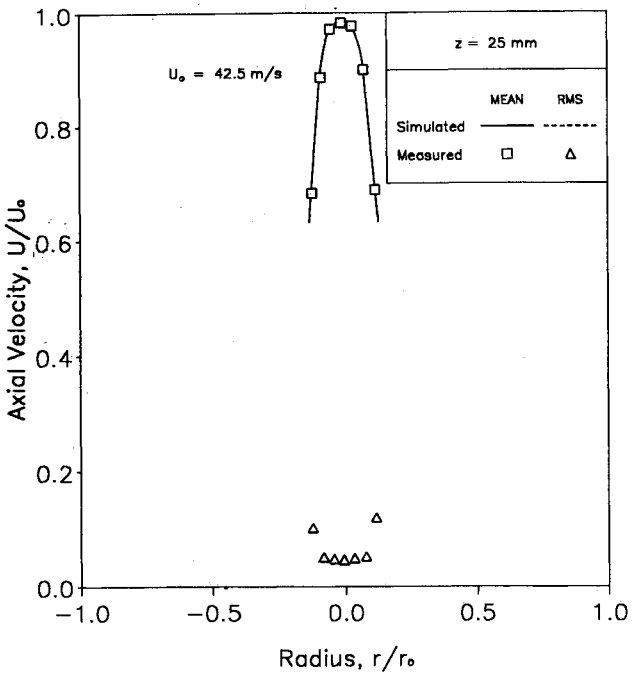

Fig. 13 Measured particle phase velocity profiles at z = 25 mm.

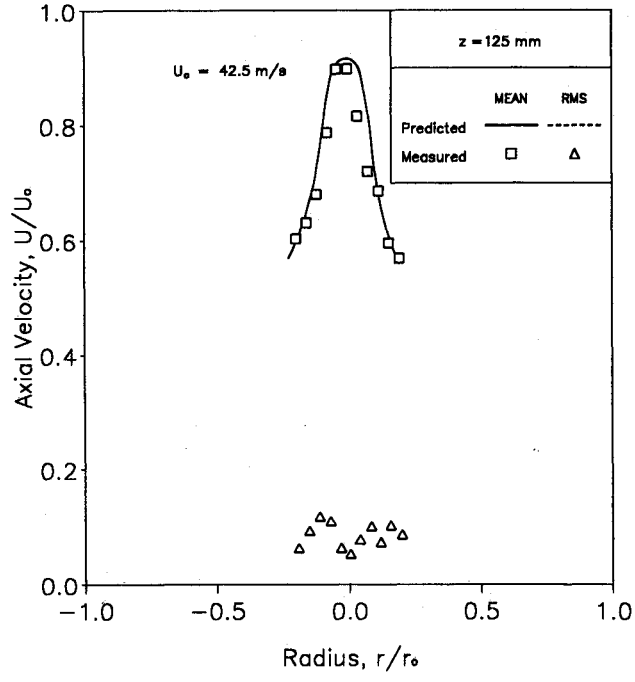

Fig. 14 Measured vs predicted particle phase velocity profiles at z = 125 mm.

simple mathematical model used to describe the turbulent diffusion of the gaseous species.

The measured axial mean and fluctuating gas velocity profiles at a distance of 25 mm from the inlet plane are shown in Fig. 10. Smoothed profiles based on the measurement values were fed as inlet conditions in the computer simulation. Figures 11 and 12 indicate the evolution of both predicted and measured velocity profiles at two measurement planes located at 125 and 325 mm downstream of the inlet plane, respectively. The predicted and measured values exhibit a sound agreement, though minor differences (< 7%) in the mixing region (at z = 125-mm plane) and on the centerline (at z = 325-mm plane) are observed. This is probably due to the fact that the adopted conventional boundary conditions for the turbulence equations on the symmetry axis do not

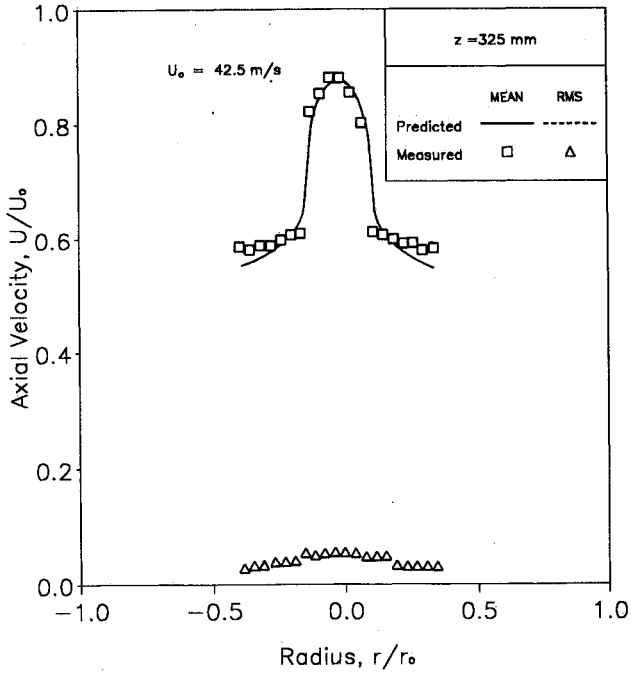

Fig. 15 Measured vs predicted particle phase velocity profiles at z = 325 mm.

satisfactorily describe the behavior of the flow. On the other hand, the limited accuracy (~5%) of the LDV system at processing low amplitude and signal-to-noise ratio signals originating from very small tracking particles might also have contributed to the aforementioned discrepancies. Although with slightly larger differences than that of the mean velocity component, the general pattern of the fluctuating velocities is in nice agreement with predicted profiles.

The mean and fluctuating particle velocity profiles measured at the same initial plane (z = 25 mm) are shown in Fig. 13. The evolution of the velocity profiles at the two downstream locations (z = 125 and 325 mm) is presented in Figs. 14 and 15, respectively. The predicted and measured particle mean velocity values are very close (maximum absolute difference is < 5%), indicating the adequacy of the physical model and the measurement technique employed. No comparison was made between the fluctuating particle velocity values as this component was not modeled in the numerical simulations.

Conclusions

An experimental investigation on ducted mixing of coaxial two-phase jets, characteristic of the flowfield in a ram combustor, has been described. The measured pressure, tracer gas concentration, and two-phase velocity profiles are in close agreement with previously reported predictions of a numerical simulation. The differences between the measured and predicted velocity values are relatively small when considering all potential error sources. This indicates that the measurement techniques used, including the two-phase LDV system, are appropriate for such studies.

It is noted that the extent of mixing between the primary and secondary flows is not considered as satisfactory. This is due to the rather simple geometry chosen to facilitate the basic experimental study and preliminary model evaluations. Therefore, there is need to explore more complex combustor geometries if enhanced mixing is sought.

References

[1]Schadow, K. C., "Boron Combustion Characteristics in Ducted Rockets," *Combustion Science and Technology*, Vol. 5, 1972, pp. 107–117.

[2]Schadow, K. C., "Study of Gas Phase Reactions in Particle Laden, Ducted Flows," *AIAA Journal*, Vol. 11, No. 7, 1973, pp. 1042–1044.

[3]Schadow, K. C., "Fuel-Rich, Particle Laden Plume Combustion," AIAA Paper 75–245, Jan. 1975.

[4]Schadow, K. C., Lee, M. C., and Wilson, K. J., "Turbulent Mixing and Combustion of Multi-Phase Reacting Flows in Ramjet and Ducted Rocket Environment," Air Force Office of Scientific Research, Naval Weapons Center, China Lake, CA, AFOSR-TR-82-0150, March 1982.

[5]Smoot, L. D., and Anderson, G. S., "Boron Particle Nonequilibrium Effects in Combusting Ducted Flows," *AIAA Journal*, Vol. 10, No. 7, 1972, pp. 857–858.

[6]Smoot, L. D., and Fort, L. A., "Confined Jet Mixing with Nonparallel Multiple-Port Injection," *AIAA Journal*, Vol. 14, No. 4, 1976, pp. 419–420.

[7]Miller, W., McClendon, S., and Burkes, W., "Design Approaches for Variable Flow Ducted Rockets," AIAA Paper 81–1489, July 1981.

[8]Choudhury, P. R., "Characteristics of a Side Dump Gas Generator Ramjet," AIAA Paper 82–1258, June 1982.

[9]Streby, G. D., "Multi-Ducted Inlet Combustor Research and Development," Aero Propulsion Lab., Air Force Wright Aeronautical Lab, Wright-Patterson AFB, OH, AFWAL-TR-83-2081, Nov. 1983.

[10]Ishikawa, N., "Experimental Study of Jet Mixing Mechanisms in a Model Secondary Combustor," *AIAA Journal*, Vol. 21, No. 4, 1983, pp. 565–570.

[11]Stull, F. D., Craig, R. R., Streby, G. D., and Vanka, S. P., "Investigation of a Dual Inlet Side Dump Combustor Using Liquid Fuel Injection," *Journal of Propulsion and Power*, Vol. 1, No. 1, Jan. 1985, pp. 83–88.

[12]Curtet, R., "Confined Jets and Recirculation Phenomena with Cold Air," *Combustion and Flame*, Vol. 2, 1958, pp. 383–411.

[13]Chigier, N. A., and Beér, J. M., "The Flow Region near the Nozzle in Double Concentric Jets," *Journal of Basic Engineering*, Dec. 1964, pp. 797–804.

[14]Peters, C. E., Phares, W. J., and Cunningham, T. H. M., "Theoretical and Experimental Studies of Ducted Mixing and Burning of Coaxial Streams," *Journal of Spacecraft and Rockets*, Vol. 6, No. 12, 1969, pp. 1435–1441.

[15]Ghia, K. N., Torda, T. P., and Lavan, Z., "Turbulent Mixing in the Initial Region of Heterogeneous Axisymmetric Coaxial Confined Jets," NASA CR-1615, May 1970.

[16]Tufts, L. W., and Smoot, L. D., "A Turbulent Mixing Coefficient Correlation for Coaxial Jets With and Without Secondary Flows," *Journal of Spacecraft and Rockets*, Vol. 8, No. 12, 1971, pp. 1183–1190.

[17]Razinsky, E., and Brighton, J. A., "A Theoretical Model for Nonseparated Mixing of a Confined Jet," *Journal of Basic Engineering*, Sept. 1972, pp. 551–558.

[18]Migdal, D., and Agosta, V. D., "A Source Model for Continuum Gas-Particle Flow," *Journal of Applied Mechanics*, Dec. 1967, pp. 860–865.

[19]Genovese, J., Edelman, R. B., and Fortune, O. F., "Some Aspects of Two-Phase Flows with Mixing and Combustion in Bounded and Unbounded Flows," *Journal of Spacecraft and Rockets*, Vol. 8, No. 4, 1971, pp. 352–357.

[20]DiGiacinto, M., Sabetta, F., and Piva, R., "Two-Way Coupling Effects in Dilute Gas-Particle Flows," *Journal of Fluids Engineering*, Vol. 104, 1982, pp. 304–312.

[21]Albagli, D., and Levy, Y., "Prediction of Two-Phase Flowfield in Ram Combustors," *Journal of Thermophysics and Heat Transfer*, Vol. 4, No. 2, April 1990, pp. 170–179.

[22]Durst, F., Melling, A., and Whitelaw, J. H., *Principles and Practice of Laser Doppler Anemometry*, Academic, London, 1981.

[23]Levy, Y., and Timnat, Y. M., "Two Phase Flow Measurements Using a Modified Laser Doppler Anemometry System," *Progress in Astronautics and Aeronautics: Single and Multiphase Flow in Electromagnetic Field: Energy, Metallurgical and Solar Applications*, Vol. 100, edited by H. Branover, M. Monds, and P. S. Lykudis, AIAA, New York, 1985, pp. 355–367.

[24]Levy, Y., and Timnat, Y. M., "Laser Techniques for Measurements of Size and Velocities of Individual Drops in Combustion Systems," *Israel Journal of Technology*, Vol. 23, 1986, pp. 93–99.

[25]Levy, Y., "On-Axis Phase Doppler Anemometry," Technion, Haifa, Israel, Aeronautical Engineering Rept., 615, Nov. 1987.

[26]Saffman, M., "Optical Particle Sizing Using the Phase of LDA Signals," Dantec Information, Measurement and Analysis, Sept. 1987.

[27]Bachalo, W. D., and Houser, M. J., "Phase/Doppler Spray Analyser for Simultaneous Measurements of Drop Size and Velocity Distributions," *Optical Engineering*, Vol. 25, No. 5, 1984, pp. 583–590.

[28]Bauckhage, K., and Floegel, H. H., "Simultaneous Measurements of Droplet Size and Velocity in Nozzle Spray," *Proc. 2nd International Symposium on Applications of Laser Anemometry to Fluid Mechanics*, Lisbon, July 1984.

[29]Gouesbet, G., Grehan, G., and Kleine, R., "Simultaneous Optical Measurement of Velocity and Size of Individual Particles," *Proc. 2nd International Symposium on Applications of Laser Anemometry to Fluid Mechanics*, Lisbon, July 1984.

[30]Durst, F., and Zare, M., "Phase Doppler Measurements in Two Phase Flow," Univ. of Karlsruhe, Karlsruhe, Germany, SFB 80/TM/63, July 1975.

[31]Yule, A. J., Chigier, N. A., Atakan, S., and Ungut, A., "Particle Size and Velocity Measurements by Laser Anemometry," *Journal of Energy*, Vol. 1, No. 4, 1978, pp. 220–228.

[32]Yule, A. J., Ah-Seng, C., Felton, P. G., Ungut, A., and Chigier, N. A., "A Study of Vaporizing Fuel Sprays by Laser Techniques," *Combustion and Flame*, Vol. 44, 1982, pp. 71–84.

[33]Yule, A. J., Ereaut, P. R., and Ungut, A., "Droplet Sizes and Velocities in Vaporizing Sprays," *Combustion and Flame*, Vol. 54, 1983, pp. 15–22.

[34]Mizutani, Y., Kodama, H., and Miyasaka, K., "Doppler-Mie Combination Technique for Determination of Size-Velocity Correlation of Spray Droplets," *Combustion and Flame*, Vol. 44, 1982, pp. 85–95.

[35]Levy, Y., Laredo, D., Albagli, D., and Timnat, Y. M., "Two Phase Flow Diagnostics in Propulsion Systems," Proc. 11th ICIASF Congress, Stanford, 1985.

[36]Levy, Y., and Lockwood, F. C., "Velocity Measurements in a Particle Laden Turbulent Free Jet," *Combustion and Flame*, Vol. 40, 1981, pp. 333–339.

[37]Hess, C. F., "Nonintrusive Optical Single-Particle Counter for Measuring the Size and Velocity of Droplets in a Spray," *Applied Optics*, Vol. 23, No. 23, 1984, pp. 4375–4382.

[38]Chedaille, J., and Braud, Y., "Measurements in Flames," *Industrial Flames*, Vol. 1 edited by J. M. Beér and M. W. Thring, Arnold, London, 1972.